The Shift of the Northern Node of the NAO and Cyclonic Rossby Wave Breaking

YI-HUI WANG AND GUDRUN MAGNUSDOTTIR

University of California, Irvine, Irvine, California

(Manuscript received 12 October 2011, in final form 12 May 2012)

ABSTRACT

Several studies have found an eastward shift in the northern node of the North Atlantic Oscillation (NAO) during the winters of 1978–97 compared to 1958–77. This study focuses on the connection between this shift of the northern node of the NAO and Rossby wave breaking (RWB) for the period 1958–97. It is found that the region of frequent cyclonic RWB underwent a northeastward shift at high latitudes in the latter 20-yr period. On a year-to-year basis, the cyclonic RWB region moves along a southwest–northeast (SW–NE)-directed axis. Both latitude and longitude of the winter maximum frequency of cyclonic RWB occurrence are positively correlated with the NAO index.

To investigate the role of location of cyclonic RWB in influencing the NAO pattern, the geographical location of frequent cyclonic RWB is divided into two subdomains located along the SW–NE axis, to the south (SW domain) and east (NE domain) of Greenland. Two composites are assembled as one cyclonic RWB occurrence is detected in one of the two subdomains in 6-hourly instantaneous data. The forcing of the mean flow due to cyclonic RWB within individual subdomains is found to be locally restricted to where the breaking occurs, which is usually near the jet exit region and far removed from the jet core. The difference in the jet between the NE and SW composites resembles the difference in the mean jet between the 1978–97 and 1958–77 periods, which suggests that the change in cyclonic RWB occurrence in the two subdomains is associated with the wobbling of the jet on the decadal time scale.

1. Introduction

The North Atlantic Oscillation (NAO) is the most pronounced climate pattern in the North Atlantic in winter, dominating its weather and climate and that of the surrounding continents. For each application, the NAO is taken to have a fixed spatial structure consisting of an anticorrelated dipole in the pressure field, with the negative node located close to Iceland and the positive node close to the Azores. The change in polarity of the NAO can be characterized by the displacement of the North Atlantic jet. When the NAO is in its positive polarity, the jet is shifted poleward. The jet moves equatorward and takes on a more zonal configuration when the NAO is in its negative polarity.

The NAO is an eddy-driven pattern of atmospheric variability with an intrinsic life cycle of approximately 10 days (Feldstein 2003). It is closely linked to Rossby wave breaking (RWB) (e.g., Strong and Magnusdottir 2008b, hereafter SM08b), where RWB refers to the irreversible and fast overturning of potential vorticity (PV) contours on isentropic surfaces (McIntyre and Palmer 1983). RWB is classified into anticyclonic and cyclonic RWB depending on the direction in which the PV contours turn (e.g., SM08b; Riviere 2009).

The relationship between RWB and the NAO on intraseasonal time scales has received much attention in the past few years (e.g., Riviere and Orlanski 2007; Strong and Magnusdottir 2008a; SM08b; Woollings et al. 2008; Riviere 2009). The type of RWB that takes place in a certain location is primarily associated with the horizontal shear of the flow (e.g., Thorncroft et al. 1993). Thus, the anticyclonic (cyclonic) side of the jet favors anticyclonic (cyclonic) RWB. Both types of RWB project on the NAO and may force the mean flow. The relationship between RWB and the NAO is significant across different time scales. For example, interannual variability of the NAO is significantly correlated with RWB occurrence within limited specified regions (SM08b).

For practical applications, the spatial pattern of the wintertime NAO is assumed to be fixed and temporal

Corresponding author address: Yi-Hui Wang, Department of Earth System Science, University of California, Irvine, Irvine, CA 92697-3100.
E-mail: yihuiw@uci.edu

DOI: 10.1175/JCLI-D-11-00596.1

variability is assessed by the NAO index. However, a displacement in the wintertime [December–March (DJFM)] pattern on the multiyear time scale has been known for some time (e.g., Hilmer and Jung 2000; Jung et al. 2003). The studies show that the northern center of action of the NAO was shifted significantly eastward during winters in 1978–97 compared to winters in 1958–77. The displacement of the center of action has been linked to the variation of Arctic sea ice export (Hilmer and Jung 2000; Jung and Hilmer 2001) as well as surface temperature and storm activity over the North Atlantic sector (Lu and Greatbatch 2002; Polyakova et al. 2006). The connection between the shift in the NAO pattern and the different variables is robust across different datasets, which implies that the shift is real and has a physical significance.

Possible reasons for the displacement of the northern node of the NAO have been addressed by previous studies. Ulbrich and Christoph (1999) find an eastward shift in the northern node of the NAO when increasing the concentration of greenhouse gases in a global climate model. Peterson et al. (2003) find that the NAO pattern shifts eastward when the NAO index is extremely positive and shifts westward when the NAO index is extremely negative. They suggest that the eastward movement of the NAO results from the positive trend in the NAO index during the latter period, which they associate with nonlinear dynamics. Luo et al. (2010) found in an idealized barotropic model that topography and variation in the latitudinal location of the jet can force a shift of the eddy-driven NAO-like anomaly. They also indicate that the longitudinal location of eddies relative to the initial NAO can shift the NAO in longitude such that the more eastward located eddies lead to an eastward shift of the NAO. Other studies have attributed the shift in the NAO to a change in the frequency distribution of different climate regimes (Cassou et al. 2004; Johnson et al. 2008).

Even though the role of eddies in the spatial shift of the NAO has been examined, to our knowledge the association of the region of frequent RWB to the shifting NAO pattern has not been explored to date. We are interested in the following: 1) Does the spatial pattern of winter-mean frequency of RWB have a decadal signature? 2) Does the shift in the northern node of the NAO correspond to a signature of change in the spatial pattern of winter-mean frequency of RWB? We will show that the displacement in frequency of cyclonic RWB resembles the shift in the spatial pattern of the NAO during the same analysis period (eastward shift in 1978–97 compared to 1958–77). We will show that the cyclonic RWB region shifted not only in the zonal direction (eastward) but also in the meridional direction (northward) from the earlier to the later 20-yr period. Following these results, the potential influence of the southwest–northeast (SW–NE) shift of cyclonic RWB on the dynamical fields and plausible physical mechanisms for this shift are discussed.

The paper is organized as follows: Data and methods are outlined in section 2. The decadal shift in the region of cyclonic RWB and the similarity to the decadal shift in the northern node of the NAO are shown in section 3. The interannual variability in the location of frequent cyclonic RWB is presented in section 4. Section 5 presents a composite analysis for cyclonic RWB in two key locations, and section 6 compares the difference in zonal wind between the two composites and the difference in zonal wind between the two 20-yr periods. Conclusions follow in section 7.

2. Data and methods

a. Data

The winter (DJFM) NAO index based on normalized sea level pressure (SLP) difference between Lisbon and Stykkisholmur/Reykjavik was downloaded from http://www.cgd.ucar.edu/cas/jhurrell/indices.html. The NAO index data is provided by the Climate Analysis Section, National Center for Atmospheric Research (NCAR), Boulder, Colorado (Hurrell 1995). Other data used in the study are taken from the National Centers for Environmental Prediction (NCEP)–National Center for Atmospheric Research reanalysis dataset on a $2.5° \times 2.5°$ latitude–longitude grid (Kistler et al. 2001). Monthly SLP is used to show the displacement of the spatial pattern of the NAO between 1978–97 and 1958–77. Monthly SLP anomalies for each of the 20-yr periods are deseasonalized by subtracting the mean over the period from monthly data. RWB is detected using the detection algorithm introduced in SM08b on the instantaneous field of NCEP 6-hourly PV. SM08b found that the 350-K isentropic surface was optimal for detecting tropospheric RWB (both cyclonic and anticyclonic) using their detection algorithm, which scans many different values of circumpolar PV contours. Other 6-hourly variables include horizontal velocity (u, v) on the 350-K isentropic surface and geopotential height of the 500-hPa isobaric surface that are used in the composite analysis. Anomalies of geopotential height and winds are deseasonalized by removing the mean over the 40 yr (1958/59–97/98) from 6-hourly data.

b. RWB detection

We adopt the methodology of SM08b to detect RWB. Here, we very briefly summarize the method. The method

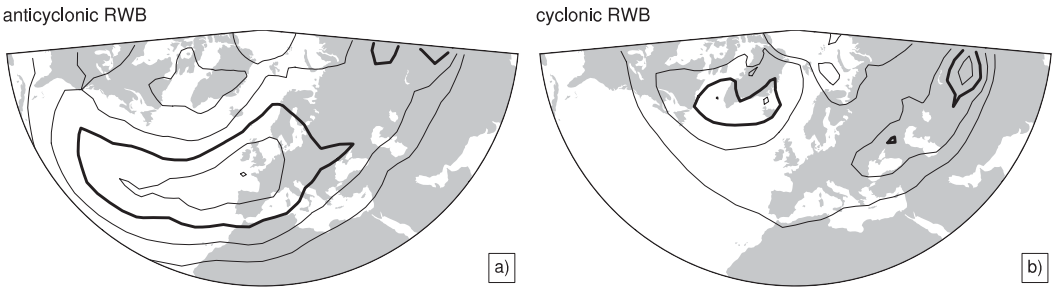

FIG. 1. Relative frequency of (a) anticyclonic RWB (γ_a) and (b) cyclonic RWB (γ_c) for DJFM for 1958/59–97/98. Contour interval is 0.02, and the bold contour is 0.06.

uses the horizontal geometry of PV contours on an isentropic surface to detect RWB. An RWB occurrence is detected if a circumpolar PV contour on the 350-K isentropic surface intersects one meridian more than once. The centroid of each RWB occurrence is recorded in latitude, longitude, and time. Anticyclonic RWB is distinguished from cyclonic RWB based on the direction of tilt of the PV tongue (see Fig. 1 in SM08b). The frequency of RWB at a specified location is quantified as the dimensionless relative frequency,

$$\gamma_a(h) \equiv \frac{1}{T}\sum_{t=1}^{T}\beta_a(h,t),$$

for anticyclonic RWB, and

$$\gamma_c(h) \equiv \frac{1}{T}\sum_{t=1}^{T}\beta_c(h,t),$$

for cyclonic RWB. The symbol h has an integer value representing one of 400 equal-area bins over the Northern Hemisphere; t is the time of one 6-hourly observation; and T is the total number of observations during the time period of interest. The symbol β_a is 1 when one anticyclonic RWB centroid is recorded in bin h at time t; otherwise, it is 0. The symbol β_c is defined in the same manner but for a cyclonic RWB occurrence. The relative frequencies of γ_a and γ_c are regridded to a resolution of $4° \times 4°$.

c. *Quantification of RWB spatial variability*

Regions of high relative frequency of RWB indicate the primary wave-breaking regions or the surf zones. The surf zones for anticyclonic and cyclonic RWB in December–February of 1958–2006 are shown in Fig. 2 in SM08b. These wave-breaking regions are almost identical to those of DJFM in 1958/59–97/98, which are shown in Fig. 1. The surf zone of cyclonic RWB in the North Atlantic (shown in Fig. 1b) is close to the south tip of Greenland on the cyclonic-shear side of the jet. To investigate the spatial variability of surf zones, the location of maximum relative frequency within the domain of interest each winter is recorded (latitude and longitude). If there are more than one local maxima of RWB relative frequency in a given winter, the one with the largest value is chosen. The time series of winter-mean latitude and longitude of maximum RWB relative frequency indicate the interannual movement of surf zones.

3. Decadal changes in the NAO pattern and the RWB regions

The centers of action (or nodes) of the NAO are located where the SLP anomalies that are associated with most of the variance in the field are located. In other words, they can be identified as the maximum standard deviation of the SLP anomaly over a given period (van Loon and Madden 1983). Comparing the standard deviation of the SLP anomaly between two periods is indicative of the change in position and intensity of the NAO action centers. The difference in standard deviation of SLP anomalies between 1978–97 and 1958–77 is shown in Fig. 2a. The dipole structure of the standard deviation difference at high latitudes indicates the eastward shift of the northern node of the NAO in the later period, which is consistent with the difference obtained when using empirical orthogonal function analysis (e.g., Jung et al. 2003). In addition to the noticeable movement of the northern center of action, the southern center of action increased in strength toward the east during the later period.

Figure 2b displays the difference in the relative frequency of anticyclonic RWB between 1978–97 and 1958–77, and Fig. 2c shows the corresponding difference for cyclonic RWB. Almost all the features in the difference fields displayed in Figs. 2b,c are statistically significant at the 95% level using a t test (not shown). Even the difference field in Fig. 2a (difference in standard deviation of SLP) shows statistical significance of

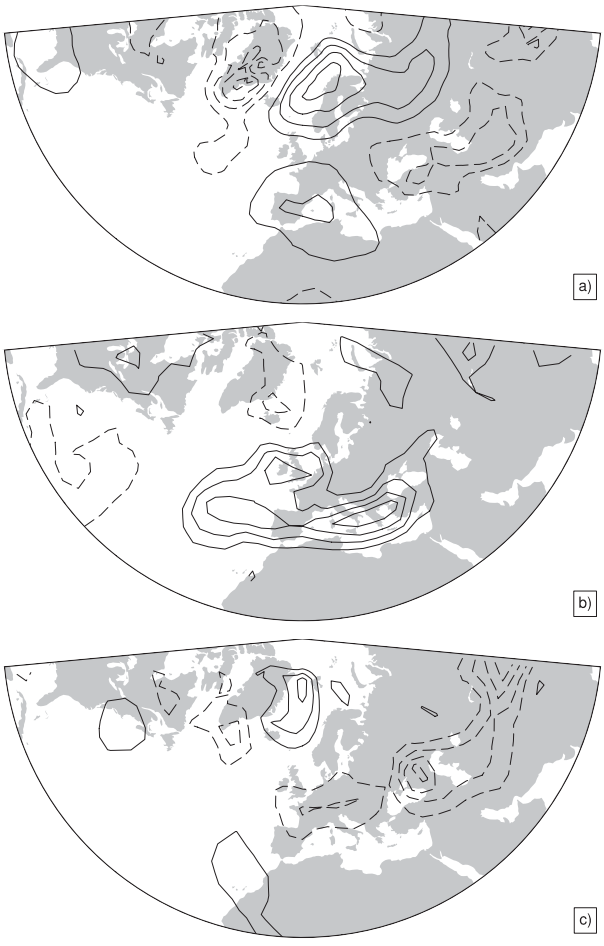

FIG. 2. Difference between December 1978–March 1998 and December 1958–March 1978 for (a) standard deviation of winter-mean sea level pressure anomalies, (b) winter-mean γ_a, and (c) winter-mean γ_c. Solid contours are positive, and dashed contours are negative. Contour interval is 0.5 hPa for (a) and 0.005 for (b),(c). The zero contour is suppressed.

the positive part of the high-latitude dipole using the *F* test but not the negative part over Greenland (not shown). Since the *F* test is very sensitive to the assumption of a normal distribution, it may be that our sample size is simply too small to satisfy this test unequivocally.

As shown in Fig. 2b, the later period had decreased anticyclonic RWB relative frequency east of Greenland and increased relative frequency farther south over the eastern North Atlantic, Western Europe, and Mediterranean regions, which are regions of high relative frequency (Fig. 1a). It is noteworthy that the northern slice of this area of increased anticyclonic RWB in Fig. 2b overlaps what SM08b called region A3 (see their Fig. 6a), a region wherein anticyclonic RWB strongly and positively influences the winter NAO index. Similarly, the area of reduced anticyclonic RWB to the north is overlapped by region A4 (SM08b, Fig. 6b), an area where anticyclonic RWB strongly and negatively influences the winter NAO index. Thus, both changes in anticyclonic RWB relative frequency lead to a more positive NAO index. However, the area of increased anticyclonic RWB is far from the northern node of the NAO, and the area of decreased anticyclonic RWB is not positioned close to the anticyclonic surf zone, which is located at lower latitudes. This may suggest that anticyclonic RWB is not of direct importance for the shift in the northern node of the NAO even though it influences the jet.

A dipole structure in cyclonic RWB relative frequency difference surrounds Greenland in Fig. 2c, implying that the surf zone of cyclonic RWB moved eastward in the later period. The dipole structure of cyclonic RWB relative frequency in Fig. 2c resembles that of SLP standard deviation anomalies in Fig. 2a, although the cyclonic RWB dipole structure appears meridionally tilted compared to the SLP dipole structure in Fig. 2a. Moreover, the area it covers is smaller than that of the SLP anomaly, which is consistent with vorticity perturbations being spatially smaller than corresponding geopotential perturbations. The area of increased cyclonic RWB frequency east of Greenland partly overlaps region C3 of Fig. 6a in SM08b, a region wherein cyclonic RWB frequency is positively correlated with the winter NAO index. The other (negative) side of the dipole in Fig. 2c does not correspond to a region of positive or negative correlation of cyclonic RWB frequency with the winter NAO index in SM08b. (This is the part that could not be verified as statistically significant by the *F* test.) The area of decreased cyclonic RWB in Fig. 2c over Western Europe corresponds to region C5 in SM08b, a region that is negatively correlated with the winter NAO index. All in all, the changes in the mean distribution of anticyclonic and cyclonic RWB between the two 20-yr time periods indicate the prevalence of a more positive NAO index in the later period.

Because one of our objectives is to link the shift in the northern node of the NAO to RWB, in the following we will focus on the analyses for cyclonic RWB. To assess whether the cyclonic RWB displacement has physical meaning, composite analyses are applied to meteorological fields as cyclonic RWB takes place in different locations. We make two composites, one corresponding to cyclonic RWB to the south of Greenland and another corresponding to cyclonic RWB to the east of Greenland. It should be noted that a similar composite analysis was performed for anticyclonic breaking in key regions; however, the effects on the background flow were of

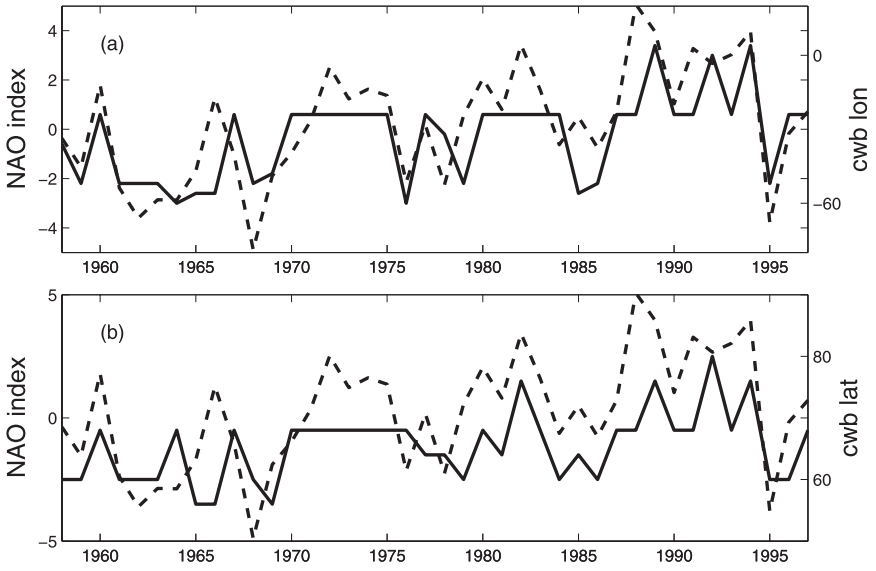

FIG. 3. (a) The longitude of maximum γ_c each winter (solid curve). (b) The latitude of maximum γ_c (solid curve). Dashed curve is the winter NAO index. The year on the x axis identifies the year of December: for example, ''1960'' means the winter of 1960/61.

secondary importance at high latitudes. We shall return to the discussion of the decadal variability of the NAO with anticyclonic RWB in the last section.

4. Relationship between the NAO index and the location of maximum cyclonic RWB frequency on an interannual time scale

The previous section addressed the possible connection between the displacement of the NAO's northern center of action and the displacement of the cyclonic RWB region between two 20-yr periods. This section focuses on the variability in the location of the cyclonic surf zone on an interannual basis within a limited area over the North Atlantic (45°–85°N, 60°W–30°E).

The time series of longitude and latitude of the point of maximum cyclonic RWB frequency each winter are compared to that of the NAO index in Fig. 3. Both the time series of latitude and longitude for maximum cyclonic RWB are significantly correlated with the observed NAO index, with correlation coefficient of 0.66 and 0.73, respectively, at 95% confidence level (t test) (Fig. 3). Small changes in the regridding of RWB relative frequency can modify the correlation slightly, but the relationship is still robust. The positive correlation suggests that, when cyclonic RWB occurs in the area to the NE, the observed NAO index should increase; when it occurs to the SW, the NAO index should decrease.

The latitude and longitude of the location of maximum cyclonic RWB relative frequency are positively correlated in time with a correlation coefficient of 0.76 (shown in Fig. 3). This indicates that the surf zone of cyclonic RWB moves along a southwest–northeast-directed axis. The maximum frequency of cyclonic RWB tends to cluster in two locations along this axis; we shall call them the NE and SW areas (displayed as bold segments in Fig. 4) in reference to their relative location along the aforementioned axis. The winter-mean location of maximum cyclonic RWB frequency (Fig. 3) shows that cyclonic RWB mainly took place in the SW region before the 1970s and took place in the NE region afterward.

5. Two composites with respect to location of cyclonic RWB

a. Composite anomalies of 500-hPa geopotential height

To investigate the influence of different horizontal locations of cyclonic RWB on the NAO pattern, we examine a composite of geopotential height at 500-hPa that is put together based on the geographic location of RWB using 6-hourly reanalysis data. The geographic locations are the NE and SW areas where cyclonic RWB tends to cluster. These two domains are separated by the average latitude and longitude of maximum γ_c over 40 winters. The NE domain (68°–80°N, 24°W–4°E) and the SW domain (56°–64°N, 56°–36°W) are depicted by the bold segments in Figs. 4a,b, respectively. Note that the NE and SW domains overlap the dipole structure of the difference in cyclonic RWB relative frequency

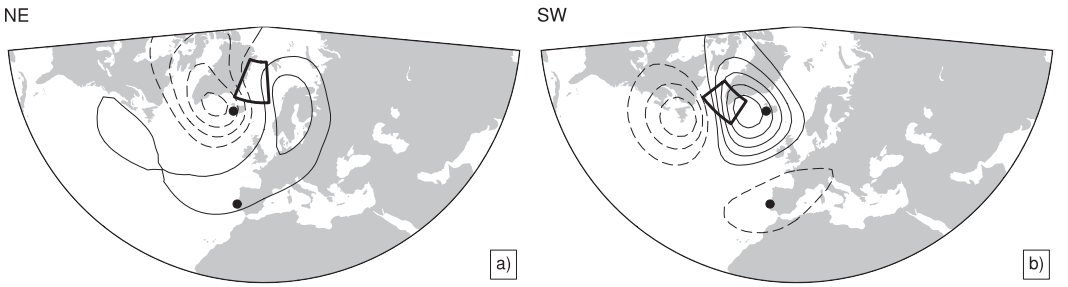

FIG. 4. The composite geopotential height anomaly at 500-hPa when one cyclonic RWB occurs within (a) the NE domain and (b) the SW domain. Solid contours are positive and dashed contours are negative. The geopotential height contours are drawn at 20-m contour intervals, and the zero contour is suppressed. The domains are indicated by the thick lines. The dots depict the two stations measuring SLP for the NAO index.

between the two periods (cf. bold segments in Fig. 4 to the dipole in Fig. 2c). During compositing, we collect the 500-hPa geopotential height anomaly at the times when a cyclonic RWB centroid is present within each of the two domains. Two composites of 500-hPa geopotential height are generated by averaging the collections, one for cyclonic RWB in the NE domain (the NE composite) and the other for cyclonic RWB in the SW domain (the SW composite). To get a clearer composite signature in the two key regions, occurrences of simultaneous cyclonic RWB in both the SW and NE domains are excluded (total of 276 occurrences). There are 2198 observational times for the NE composite and 2396 observational times for the SW composite over the 40 winters.

The composite of 500-hPa geopotential height when cyclonic RWB takes place in the NE domain is shown in Fig. 4a; the equivalent but for the SW domain is shown in Fig. 4b. Within each subregion (i.e., the centroid of RWB is located in either the NE or the SW domain), the geopotential signature of cyclonic RWB is the same or a positive anomaly to the northeast for each domain with a negative anomaly to the southwest. For the NE composite, the positive anomaly is centered over Scandinavia while the negative counterpart is located between southern Greenland and Iceland (Fig. 4a). For the SW composite, the positive anomaly is between southern Greenland and Iceland, while the negative anomaly is centered over Newfoundland (Fig. 4b). The signal is robust even though we do not collocate the different cyclonic RWB centroids before averaging over each composite. The corresponding composites in SLP show similar signatures consistent with the equivalent barotropic structure of the NAO (not shown).

Previous studies pointed out that the latitude of RWB influences the projection of its geopotential signature onto the NAO and therefore changes the polarity of the NAO (e.g., SM08b). That is, when the positive eddy-driven geopotential anomaly projects onto the southern (positive) NAO center of action and the negative eddy-driven geopotential anomaly projects onto the negative NAO center of action, the NAO polarity strengthens and the NAO index increases. When the opposite occurs, the NAO weakens and the NAO index decreases. Since the signature of cyclonic RWB in geopotential is centered in the NE and SW domains (Fig. 4), their projection onto the fixed NAO pattern can lead to different values of the NAO index depending on which domain is being considered. To interpret the influence of geopotential anomaly in different locations on the NAO index, the northern station (Stykkisholmur/Reykjavik: the northern dot in Figs. 4a,b) and the southern station (Lisbon: the southern dot in Figs. 4a,b) for defining the NAO index are marked as the centers of action of the NAO. For the NE composite, the northern station records the primarily negative geopotential anomaly while the southern station only detects the weaker positive geopotential anomaly (Fig. 4a). As a result, the difference in geopotential anomaly measured by the two stations leads to a contribution to the positive NAO index. For the SW composite, the northern station records the primarily positive geopotential anomaly, whereas the southern station only detects the weaker negative geopotential anomaly. The difference in geopotential anomaly between the two stations in this case results in a contribution to the negative NAO index.

*b. Composite anomalies of zonal wind and divergence of the **E** vector*

To understand the state of the background flow as cyclonic RWB takes place in the two different domains, we examine the composite of zonal wind on the 350-K isentropic surface in Fig. 5. We find that the jet is extended northeastward when cyclonic RWB takes place in the NE domain (contours in Fig. 5a). The jet exit is southwestward retreated when cyclonic RWB occurs in the SW domain (contours in Fig. 5b). The consistent change in location of cyclonic RWB with that of the jet

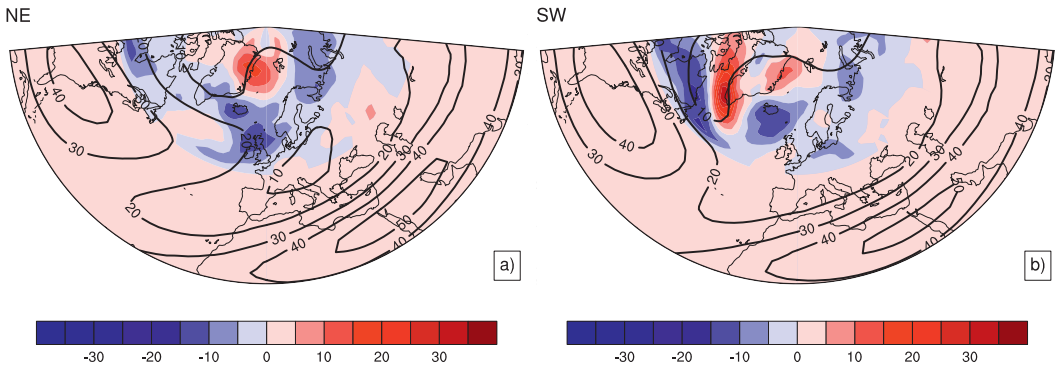

FIG. 5. The composite of zonal wind and $\partial E_y/\partial y$ on the 350-K isentropic surface when cyclonic RWB takes place within (a) the NE domain and (b) the SW domain. Contours are zonal wind (m s^{-1}; contour interval of 10 m s^{-1}), and shading is $\partial E_y/\partial y$ (10^{-5} m s^{-2}). To emphasize higher latitudes, $\partial E_y/\partial y$ is only plotted north of 50°N.

extent is in agreement with the ideas of small-amplitude Rossby wave propagation and breaking; that is, large-scale Rossby waves tend to break where the westerly background flow becomes too weak to support wave propagation (Magnusdottir and Haynes 1999).

Under quasigeostrophic scaling and using barotropic arguments, the eddy forcing on the background flow can be inferred by considering the horizontal divergence of the **E** vector (Hoskins et al. 1983). The **E** vector, $\mathbf{E} \equiv (v'^2 - u'^2, -u'v')$, where (u', v') denotes horizontal velocity anomaly from the time mean of that observation time over 40 winters. When the divergence of **E** is positive, the mean flow is accelerated by the eddies. The magnitude of the divergence of **E** is dominated by the y contribution ($\partial E_y/\partial y$) in the vicinity of the NE and SW domains. Therefore, only $\partial E_y/\partial y$ is displayed in Fig. 5. The shading in Figs. 5a,b represents the composite of $\partial E_y/\partial y$ when cyclonic RWB occurs in the NE domain and the SW domain, respectively. It indicates that cyclonic RWB within the NE domain enforces the westerlies northeast of Greenland (Fig. 5a), whereas cyclonic RWB within the SW domain accelerates the westerlies southwest of Greenland (Fig. 5b). The cyclonic RWB strengthens the divergence of momentum flux at its breaking location, which is consistent with the local effect reinforced by wave breakings in Woollings et al. (2010). The magnitude of the positive anomaly for the NE domain is weaker than that for the SW domain (shading in Fig. 5). The weaker anomaly for the NE domain could be due to the greater spatial variability of cyclonic RWB in the area and therefore smoothing when averaging over the composite. The maximum in $\partial E_y/\partial y$ is located poleward of the jet exit, which is far from the jet core but close to the northern node of the NAO. This suggests that cyclonic RWB in each domain influences the location of the northern node of the NAO, keeping it to the east when the breaking is predominantly in the NE domain and to the west when in the SW domain.

6. Relationship between decadal change in jet variability and cyclonic RWB occurrence

To some degree the NAO index is a measure of the wobbling of the North Atlantic jet. When the jet shifts poleward, the NAO index increases. When it shifts equatorward, the NAO index decreases. Because the earlier period had a more negative NAO index compared with the later period (Peterson et al. 2003), the jet extended farther poleward in the later period. We expect that the poleward-shifted jet in the later period is similar to the composite jet when cyclonic RWB takes place in the NE domain (contours in Fig. 5a), and the jet in the earlier period is more like the composite jet when cyclonic RWB takes place in the SW domain (contours in Fig. 5b).

Figure 6a shows the difference in zonal wind between composites of cyclonic RWB in the NE domain and composites of cyclonic RWB in the SW domain. Figure 6b displays the difference in the mean zonal wind between the two 20-yr periods of 1978–97 and 1958–77. All the main features in the difference fields are statistically significant (for the absolute values greater than 2 m s^{-1}, using a t test at the 95% level; not shown). The difference between the two 20-yr winter-mean zonal wind fields is evidently similar to the difference between composites, especially the feature of increased zonal wind speed south of Greenland (around 50°N) and a zonal band of decreased zonal wind speed around 30°N. Although the magnitude of the difference for the composites is greater than that for the 20-yr averages, the similarity implies that the jet displacement on the decadal time scale goes hand in hand with enhanced likelihood of cyclonic RWB in

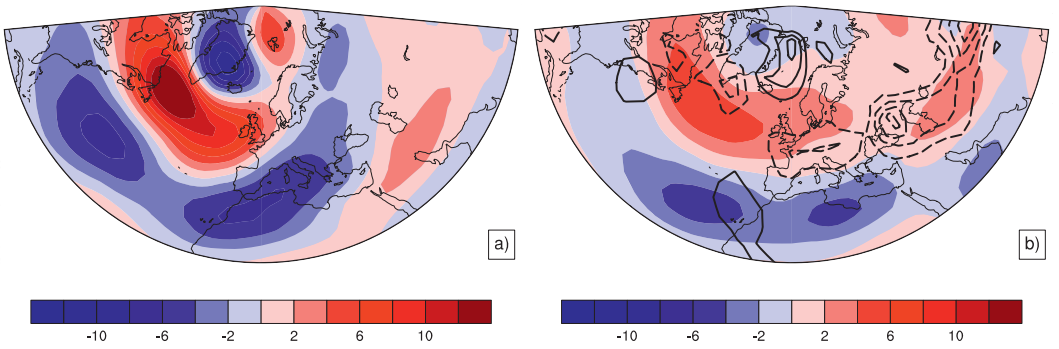

FIG. 6. In shading is the difference in zonal wind (m s^{-1}) on the 350-K isentropic surface (a) between the NE and SW domain composites and (b) between December 1978–March 1998 and December 1958–March 1978. The difference in γ_c between the two periods is superimposed as contours in (b) (as in Fig. 2c). Positive and negative values are represented as solid and dashed contours, respectively.

one domain and reduced in the other domain during the different 20-yr periods.

The change in cyclonic RWB occurrence within the NE and SW domains during different periods is found to correspond to the decadal jet displacement. There were 262 more cyclonic RWB occurrences detected in the SW domain than in the NE domain during 1958–77 (1262 occurrences in the SW and 1000 occurrences in the NE domain). There were 64 more cyclonic RWB occurrences in the NE domain during 1978–97 (1134 occurrences in the SW and 1198 occurrences in the NE domain). The increased cyclonic RWB in the SW domain in the earlier period is much greater than that in the NE domain in the latter period. The asymmetry in the number of RWB frequency may be influenced by the spherical effect of the earth that limits RWB occurrences farther poleward since there is less area because of the convergence of meridians (Barnes et al. 2010). Generally, there is a consistency between the shift in the location of cyclonic RWB occurrence and the displacement of the jet.

7. Conclusions

The present work focuses on the shift in location of the northern center of action of the NAO in 1978–97 compared to 1958–77 and the corresponding shift in location of the maximum cyclonic RWB frequency in the same general area. Different from the shifting NAO center of action, where its displacement is primarily zonal (e.g., Hilmer and Jung 2000), the shift in cyclonic RWB is along a southwest–northeast-directed axis or from the south to the east of Greenland. Previous studies only consider the effect of latitude of RWB on how it projects on the NAO. We show that cyclonic RWB in the two different locations projects differently on the NAO pattern, resulting in different responses of the NAO index.

To investigate the signature in the dynamical fields associated with different locations of cyclonic RWB, we divide the surf zone of cyclonic RWB in the North Atlantic into two subdomains: one is located northeast of its mean location (NE domain) and another is located southwest of its mean location (SW domain). A composite analysis that classifies cyclonic RWB depending on the location of the RWB centroid shows that when cyclonic RWB occurs within the NE domain it will result in a positive NAO and when it occurs within the SW domain it will result in a negative NAO. This composite result helps explain the positive correlation between the latitude/longitude of cyclonic RWB maximum relative frequency in the North Atlantic and the NAO index on an interannual time scale. The composite of zonal wind and $\partial E_y/\partial y$ in the upper troposphere, corresponding to cyclonic RWB taking place in either the NE domain or the SW domain is also examined. The result shows that the location of cyclonic RWB and the location of the jet are closely tied. Cyclonic RWB has a rather local effect on the wind field on the cyclonic side of the jet exit, which is also close to the northern node of the NAO. This is suggestive of cyclonic RWB tending to maintain the northern node of the NAO near to where cyclonic RWB is occurring, which is closely tied to the background flow.

SM08b modeled the interannual variability in the NAO index by a multiple linear regression model where the five predictors are based on winter-mean wave-breaking frequencies in five specific regions, where three correspond to anticyclonic breaking and two correspond to cyclonic breaking. They find that the fit is very good for the 47 seasons. Even including only the most important predictor or that associated with anticyclonic breaking frequency in the main region shown in Fig. 1a gives a good fit. We find that the change in the location of anticyclonic RWB occurrences (Fig. 2b)

between the two 20-yr periods corresponds to a more positive NAO index in the later period. The increased anticyclonic RWB occurrences in the later period were located between Western Europe and the Mediterranean region, which partly overlap with the location of the anticyclonic surf zone. To examine the connection between the changing location of anticyclonic RWB and the shift of the northern node of the NAO, we performed the same type of composite analysis as before, now to the geopotential height and wind fields when anticyclonic RWB takes place over Western Europe and the Mediterranean region. We found no signature of forcing by anticyclonic RWB onto the background flow near the northern node of the NAO (not shown). The result suggests that the increased anticyclonic RWB in the later period has no direct relevance to the shift in the northern node of the NAO; however, it is important in forcing the jet and thus may have indirect influence since as described above the location of cyclonic breaking is sensitive to the location of the jet exit.

Recently, after this paper was submitted for publication, we examined variability in the spatial structure of the NAO over multiple 20-yr periods (Wang et al. 2012). We find that there is also considerable movement in the southern node of the NAO. It is quite possible that anticyclonic breaking has a direct impact on this variability similar to the cyclonic breaking influencing the location of the northern node of the NAO as described in the current paper.

The change in location of high-latitude North Atlantic cyclonic RWB occurrences influences the location of the northern node of the NAO on the decadal time scale. It also influences the value of the NAO index (based on the standard NAO pattern) on decadal time scales. By contrast, in the Southern Hemisphere, the change in cyclonic RWB occurrences plays a minor role in the variability of the southern annular mode (SAM) index during December–February over the past three decades (Wang and Magnusdottir 2011). It is anticyclonic RWB frequency that shows a robust positive trend and similar interannual and intraseasonal variations as the SAM index.

The composite of zonal wind suggests that the location of cyclonic RWB is tied to the location of the jet exit. This relationship between cyclonic RWB and jet extension still holds on the decadal time scale as seen by comparing the composites to the results over the two 20-yr periods. We find that the spatial pattern of the difference in zonal wind between the two 20-yr periods of 1978–97 and 1958–77 is similar to that of the difference between the NE composite and the SW composite (Fig. 6). The difference in cyclonic RWB occurrence in the NE and SW domains between the two 20-yr periods corresponds closely to the change in jet extension during the same periods. Therefore, it is likely that the northeast shift in the cyclonic RWB surf zone during 1978–97 is governed by the extension of the jet exit. On the other hand, the increased cyclonic RWB in the NE domain during 1978–97 can accelerate the mean flow locally, possibly prolonging the presence of the northern node of the NAO in this eastward-shifted location. This study presents results regarding the shift of the northern node of the NAO based on observations. We are unable to separate cause and effect concerning this shift and exactly which is causing it, the shift in cyclonic RWB or the extension/contraction of the jet. Rather, we consider the eddy–mean flow interaction together as mutually compensating processes. There are other possible mechanisms driving the jet shift on decadal time scales, including decadal variability of the Atlantic meridional overturning circulation (e.g., Msadek et al. 2011), decadal change in the frequency of tropical intraseasonal precipitation events (e.g., Yuan et al. 2011), and decadal change in solar variability (e.g., Ineson et al. 2011).

Acknowledgments. We thank Hal Stern, Yaming Yu, and Xian Tian for helpful discussions and Ashley Payne for proofreading a previous version of the manuscript. Finally, we thank three reviewers for comments on the previous version of the manuscript. This work is supported by NSF Grant AGS-1025374 and NOAA Grant NA09OAR4310132.

REFERENCES

Barnes, E. A., D. L. Hartmann, D. M. W. Frierson, and J. Kidston, 2010: Effect of latitude on the persistence of eddy-driven jets. *Geophys. Res. Lett.,* **37,** L11804, doi:10.1029/2010GL043199.

Cassou, C., L. Terray, J. W. Hurrell, and C. Deser, 2004: North Atlantic winter climate regimes: Spatial asymmetry, stationarity with time, and oceanic forcing. *J. Climate,* **17,** 1055–1068.

Feldstein, S. B., 2003: The dynamics of NAO teleconnection pattern growth and decay. *Quart. J. Roy. Meteor. Soc.,* **129,** 901–924.

Hilmer, M., and T. Jung, 2000: Evidence for a recent change in the link between the North Atlantic Oscillation and Arctic sea ice export. *Geophys. Res. Lett.,* **27,** 989–992.

Hoskins, B. J., I. N. James, and G. H. White, 1983: The shape, propagation and mean-flow interaction of large-scale weather systems. *J. Atmos. Sci.,* **40,** 1595–1612.

Hurrell, J. W., 1995: Decadal trends in the North Atlantic Oscillation: Regional temperatures and precipitation. *Science,* **269,** 676–679.

Ineson, S., A. A. Scaife, J. R. Knight, J. C. Manners, N. J. Dunstone, L. J. Gray, and J. D. Haigh, 2011: Solar forcing of winter climate variability in the Northern Hemisphere. *Nat. Geosci.,* **4,** 753–757.

Johnson, N. C., S. B. Feldstein, and B. Tremblay, 2008: The continuum of Northern Hemisphere teleconnection patterns and a description of the NAO shift with the use of self-organizing maps. *J. Climate,* **21,** 6354–6371.

Jung, T., and M. Hilmer, 2001: The link between the North Atlantic Oscillation and Arctic sea ice export through Fram Strait. *J. Climate,* **14,** 3932–3943.

——, ——, E. Ruprecht, S. Kleppek, S. K. Gulev, and O. Zolina, 2003: Characteristics of the recent eastward shift of interannual NAO variability. *J. Climate,* **16,** 3371–3382.

Kistler, R., and Coauthors, 2001: The NCEP–NCAR 50-Year Reanalysis: Monthly means CD-ROM and documentation. *Bull. Amer. Meteor. Soc.,* **82,** 247–267.

Lu, J., and R. J. Greatbatch, 2002: The changing relationship between the NAO and Northern Hemisphere climate variability. *Geophys. Res. Lett.,* **29,** 1148, doi:10.1029/2001GL014052.

Luo, D. H., L. H. Zhong, R. C. Ren, and C. Z. Wang, 2010: Spatial pattern and zonal shift of the North Atlantic Oscillation. Part II: Numerical experiments. *J. Atmos. Sci.,* **67,** 2827–2853.

Magnusdottir, G., and P. H. Haynes, 1999: Reflection of planetary waves in three-dimensional tropospheric flows. *J. Atmos. Sci.,* **56,** 652–670.

McIntyre, M. E., and T. N. Palmer, 1983: Breaking planetary-waves in the stratosphere. *Nature,* **305,** 593–600.

Msadek, R., C. Frankignoul, and L. Z. X. Li, 2011: Mechanisms of the atmospheric response to North Atlantic multidecadal variability: A model study. *Climate Dyn.,* **36,** 1255–1276.

Peterson, K. A., J. Lu, and R. J. Greatbatch, 2003: Evidence of nonlinear dynamics in the eastward shift of the NAO. *Geophys. Res. Lett.,* **30,** 1030, doi:10.1029/2002GL015585.

Polyakova, E. I., A. G. Journel, I. V. Polyakov, and U. S. Bhatt, 2006: Changing relationship between the North Atlantic Oscillation and key North Atlantic climate parameters. *Geophys. Res. Lett.,* **33,** L03711, doi:10.1029/2005GL024573.

Riviere, G., 2009: Effect of latitudinal variations in low-level baroclinicity on eddy life cycles and upper-tropospheric wave-breaking processes. *J. Atmos. Sci.,* **66,** 1569–1592.

——, and I. Orlanski, 2007: Characteristics of the Atlantic storm-track eddy activity and its relation with the North Atlantic Oscillation. *J. Atmos. Sci.,* **64,** 241–266.

Strong, C., and G. Magnusdottir, 2008a: How Rossby wave breaking over the Pacific forces the North Atlantic Oscillation. *Geophys. Res. Lett.,* **35,** L10706, doi:10.1029/2008GL033578.

——, and ——, 2008b: Tropospheric Rossby wave breaking and the NAO/NAM. *J. Atmos. Sci.,* **65,** 2861–2876.

Thorncroft, C. D., B. J. Hoskins, and M. F. McIntyre, 1993: Two paradigms of baroclinic-wave life-cycle behavior. *Quart. J. Roy. Meteor. Soc.,* **119,** 17–55.

Ulbrich, U., and M. Christoph, 1999: A shift of the NAO and increasing storm track activity over Europe due to anthropogenic greenhouse gas forcing. *Climate Dyn.,* **15,** 551–559.

van Loon, H., and R. A. Madden, 1983: Interannual variations of mean monthly sea-level pressure in January. *J. Climate Appl. Meteor.,* **22,** 687–692.

Wang, Y.-H., and G. Magnusdottir, 2011: Tropospheric Rossby wave breaking and the SAM. *J. Climate,* **24,** 2134–2146.

——, ——, H. Stern, X. Tian, and Y. Yu, 2012: Decadal variability of the NAO—Introducing an augmented NAO index. *Geophys. Res. Lett.,* doi:10.1029/2012GL053413, in press.

Woollings, T., B. Hoskins, M. Blackburn, and P. Berrisford, 2008: A new Rossby wave-breaking interpretation of the North Atlantic Oscillation. *J. Atmos. Sci.,* **65,** 609–626.

——, A. Hannachi, and B. Hoskins, 2010: Variability of the North Atlantic eddy-driven jet stream. *Quart. J. Roy. Meteor. Soc.,* **136,** 856–868.

Yuan, J. C., S. B. Feldstein, S. Lee, and B. K. Tan, 2011: The relationship between the North Atlantic jet and tropical convection over the Indian and western Pacific Oceans. *J. Climate,* **24,** 6100–6113.